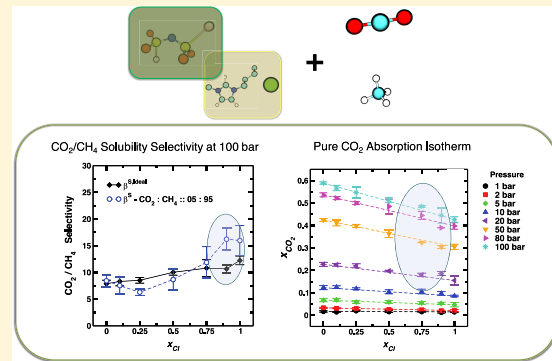


Monte Carlo Simulations of Pure and Mixed Gas Solubilities of CO_2 and CH_4 in Nonideal Ionic Liquid–Ionic Liquid Mixtures

Utkarsh Kapoor¹ and Jindal K. Shah^{*1,2}¹ School of Chemical Engineering, Oklahoma State University, Stillwater, Oklahoma 74078, United States² Supporting Information

ABSTRACT: The knowledge of mixed gas solubility in ionic liquids at high pressures, which becomes relevant in applications such as tertiary oil recovery and landfill gas utilization, is critical for the design of gas separation technologies. In this study, we examine ionic liquid mixtures for tuning the solubility of carbon dioxide (CO_2) and methane (CH_4). Using Gibbs ensemble Monte Carlo simulations, absorption isotherms of pure CO_2 and CH_4 are computed in the binary ionic liquid mixtures containing the common cation 1-*n*-butyl-3-methylimidazolium [C_4mim]⁺ and the anions chloride Cl^- and bis-(trifluoromethanesulfonyl)imide $[\text{NTf}_2]^-$ using five molar compositions at 353 K and the pressures ranging from 1 to 100 bar. Additionally, mixture gas solubilities of CO_2 and CH_4 with the starting gas phase mole ratios of 5:95 and 15:85 at a total pressure of 100 bar are determined and compared with the ideal predictions obtained from the solubilities calculated in pure ionic liquids. Results show that the mixture solubilities deviate from the ideal mixing rule at high pressures with improved solubilities in ionic liquid mixtures having up to 10% of $[\text{C}_4\text{mim}][\text{NTf}_2]$ in $[\text{C}_4\text{mim}]\text{Cl}$. Furthermore, for the entire ionic liquid mixture composition range, the CO_2/CH_4 solubility selectivities exhibited a nonlinear behavior. Interestingly, simulated CO_2/CH_4 solubility selectivities at the mole ratios of 05:95 and 15:85 do not differ significantly from the ideal solubility selectivities suggesting independent gas absorption, except for 05:95 at 10% of $[\text{C}_4\text{mim}][\text{NTf}_2]$ in $[\text{C}_4\text{mim}]\text{Cl}$. Thus, there is a potential for improving CO_2/CH_4 selectivity in pure $[\text{C}_4\text{mim}]\text{Cl}$ with the addition of a small amount of $[\text{C}_4\text{mim}][\text{NTf}_2]$ ionic liquid.



INTRODUCTION

Gas separation is one of the most important unit processes in the chemical and petrochemical industries. Contaminants in the form of acid gases such as CO_2 have negative impacts on both the quality and viability of the natural gas fields.¹ Industrially, CO_2 removal is achieved by absorbing it in volatile organic solvents such as aqueous alkanolamine, which suffers from a number of disadvantages related to the loss of solvent due to volatilization, corrosion, and high energy demand to regenerate the solvents, increasing the cost of the operation.^{2–4}

Ionic liquids have been suggested as promising gas separating agents and potential replacements for current materials.^{5–8} Room temperature ionic liquids are molten salts with melting temperatures below 100 °C. They are comprised entirely of ions—the cation is usually highly asymmetric and of organic nature, whereas the anion can be either organic or inorganic. Charge delocalization and complex structures frustrate ordered packing, lowering the melting point. One of the attractive features of ionic liquids is that the cation–anion combinations can be varied almost at will, providing considerable freedom to adjust material properties of interest for a given application. One of the vibrant research areas in the field of ionic liquids is that of gas separation, especially those involving polar and nonpolar gas mixtures such as CO_2 and CH_4 ,^{7–11} suggesting that these solvents are useful

in absorption-based separations.^{12–14} A number of research articles focused on experimental^{9,10,15–20} and computational^{8,21–24} work have been published with emphasis on gas solubility in various ionic liquids. These studies are only representative; for a thorough understanding of the field, we recommend the recently published article by Chen and co-workers²⁵ for a comprehensive collection of gas solubility research in ionic liquids.

In general, at the same temperature and pressure conditions, solubility of pure gases in ionic liquids follows the following order: SO_2 (H_2S) > CO_2 ≈ N_2O > C_2H_4 > C_2H_6 > CH_4 > Ar > O_2 > N_2 > CO > H_2 .²⁵ The ordering suggests that it might be possible to utilize ionic liquids for separating gas mixtures. It is really interesting to note that experimental studies have supported the idea that when a gas having higher solubility in ionic liquids is mixed with a gas which possesses lower solubility in ionic liquids, the gas with higher solubility enhances the other gas solubility while its own solubility is reduced.^{20,26,27} For instance, mixed gas solubility of CO_2/H_2 in

Special Issue: Chuck Eckert Festschrift

Received: June 21, 2019

Revised: August 8, 2019

Accepted: August 12, 2019

Published: August 12, 2019

70 various ionic liquids namely $[C_2\text{mim}][\text{NTf}_2]$,²⁸ $[C_4\text{mim}]\text{[PF}_6]$,¹⁵ and $[C_4\text{mim}]\text{[BF}_4]$ ²⁹ have shown an increase in 71 solubility selectivity of H_2 . On the contrary, computational 72 study involving solubility of CO_2/O_2 and SO_2/N_2 in 73 $[C_6\text{mim}]\text{[NTf}_2]$ by Shi and Maginn³⁰ does not support the 74 argument and it is speculated that the observed solubility 75 behavior can depend on the operating conditions. Further- 76 more, some authors have proposed that the presence of small 77 quantities of water in the ionic liquid sample can affect the 78 solubility behavior significantly.³¹

80 Although the topic of capturing a mixture of CO_2 and CH_4 81 simultaneously with ionic liquids is of great interest, availability 82 of the relevant data is scarce. Hert et al.²⁰ concluded that the 83 presence of CO_2 improves the solubility of CH_4 in $[C_6\text{mim}]\text{[NTf}_2]$. Computational investigation, with the need to advance 84 in supported ionic liquid membrane technology, by Budha- 85 thoki et al.²² found only slight nonideal behavior of CO_2/CH_4 86 solubility selectivity and permselectivity in bulk $[C_4\text{mim}]\text{[NTf}_2]$ 87 ionic liquid at 333 K, and thus, the authors suggested 88 that mixed gas properties can be safely estimated from pure gas 89 data under ideal assumptions. However, the same authors, in 90 another study,²³ showed that the permselectivity of CO_2 over 91 CH_4 can be enhanced by using confinement.

92 Based on our previous studies^{32,33} we believe that another 93 approach to precisely tune the gas solubilities is to consider 94 binary mixtures of ionic liquids that offer control over CO_2 95 solubility when the ionic liquid mixture composition is varied. 96 To our knowledge, the only available data for binary ionic 97 liquid mixtures is that reported by Finotello et al.³⁴ The 98 authors conducted a systematic study of the gas solubility and 99 solubility selectivity of CO_2/CH_4 in the binary mixtures of 1- 100 ethyl-3-methylimidazolium $[C_2\text{mim}]$ bis- 101 (trifluoromethanesulfonyl)imide $[\text{NTf}_2]$ and $[C_2\text{mim}]$ tetra- 102 fluoroborate $[\text{BF}_4]$. They concluded that although the 103 solubility selectivity could be described by regular solution 104 theory the ionic liquid mixtures of $[C_2\text{mim}][\text{BF}_4]_x$ $[\text{NTf}_2]_{1-x}$ 105 with $x = 0.90$ and 0.95 displayed enhanced solubility selectivity 106 for CO_2 over CH_4 .

107 In this article, we aim to provide the gas solubility data for 108 pure CO_2 and CH_4 , and their mixtures in the binary ionic 109 liquid mixtures composed of the common cation $[C_4\text{mim}]^+$ 110 paired with Cl^- and $[\text{NTf}_2]^-$. We employ the Gibbs ensemble 111 Monte Carlo approach to compute the solubility and 112 selectivity. The choice of the ionic liquid mixture is based on 113 the fact that our previous studies have shown that these ionic 114 liquid mixtures are characterized by local organization of 115 anions around the cation that differs markedly from those of 116 pure ionic liquid. The consequence of this behavior is that, 117 although the Henry's constant for CO_2 in these ionic liquid 118 mixtures is predictable from an ideal mixing rule, the 119 dissolution mechanism is different from that in the pure 120 ionic liquids.^{32,33} However, it is not clear if the local ionic 121 arrangements in these ionic liquid mixtures will impact CH_4 122 solubility and CO_2/CH_4 selectivity.

124 ■ FORCE FIELD

125 The force field parameters for carbon dioxide (CO_2) and 126 methane (CH_4) molecules were obtained from Shi and 127 Maginn²⁴ and TRAPPÉ,³⁵ respectively. Ionic liquid mixtures 128 containing the cation 1-*n*-butyl-3-methylimidazolium 129 $[C_4\text{mim}]^+$ and the anions chloride Cl^- and bis- 130 (trifluoromethanesulfonyl)imide $[\text{NTf}_2]^-$ were modeled using 131 a united atom classical force field developed by Liu and co-

workers.^{36,37} In this force field, methyl ($-\text{CH}_3$), methylene ($-\text{CH}_2-$), and trifluoromethane ($-\text{CF}_3$) groups are treated as a single interaction site, while heteroatoms such as oxygen, sulfur, and imidazolium ring hydrogen atoms, due to their importance in hydrogen bonding interactions with the anions, are modeled explicitly (schematic included in Figure S1 of the Supporting Information); and the total charge on the ion moieties is ± 0.8 . The force field was selected to be consistent with our previous studies regarding the structure and dynamics of the same binary ionic liquid mixtures³² and the calculation of Henry's constants for CO_2 in these mixtures using free energy calculations performed using the Bennett Acceptance Ratio (BAR) approach.³³ Furthermore, our recent work, where we evaluated the predictive capability of four different classical force field models for phase equilibria properties of different gases in multiple ionic liquids, also suggested that performance of force field models for gas solubility data and temperature dependent trends aligns better with experimental results for force field models with scaled noninteger charges in comparison to the integer charge models.³⁸

The intermolecular and intramolecular interactions were represented according to the following functional form:

$$E_{\text{tot}} = \sum_{\text{bonds}} K_r(r - r_0)^2 + \sum_{\text{angles}} K_\theta(\theta - \theta_0)^2 + \sum_{\text{dihedrals}} K_\chi[1 + \cos(n\chi - \delta_\chi)] + \sum_{\text{impropers}} K_\psi[1 + \cos(n\psi - \delta_\psi)] + \sum_{i=1}^{N-1} \sum_{i < j} \left\{ 4\epsilon_{ij} \left[\left(\frac{\sigma_{ij}}{r_{ij}} \right)^{12} - \left(\frac{\sigma_{ij}}{r_{ij}} \right)^6 \right] + \left(\frac{q_i q_j}{r_{ij}} \right) \right\} \quad (1) \quad 154$$

The energetic contributions due to bonds, angles, dihedrals, and improper torsions are described by the terms involving K_r , K_θ , K_χ , and K_ψ , respectively. The Lennard-Jones (LJ) 12–6 potential is used to express van der Waals interactions, for which ϵ_{ij} and σ_{ij} denote the size and energy parameters between atoms i and j . q_i and q_j are the partial charges placed on the atomic sites i and j , respectively, and describe the electrostatic interactions in the system via the Coulomb's law. As proposed for the model, the Lorentz–Berthelot combining rule was used to compute interactions between two different atom types. Intramolecular interactions between the terminal atoms in a dihedral, the so-called 1–4 interactions, were scaled by a factor of 0.5 for both the LJ and electrostatic interactions, while the nonbonded interactions between the atoms connected by bonds and angles were excluded.³⁷

■ SIMULATION DETAILS

The absorption isotherms of CO_2 and CH_4 and their mixtures in the binary ionic liquid mixture system of $[C_4\text{mim}] \text{Cl}_x$ ($x = 0.0, 0.10, 0.25, 0.5, 0.75, 0.90, 1.0$) were computed using the isothermal–isobaric Gibbs ensemble Monte Carlo (GEMC-NPT) approach as implemented in the CASSANDRA package.³⁹ Pure gas solubilities were calculated at pressures ranging from 1 to 100 bar (specifically; 1, 2, 5, 10, 20, 50, 80, and 100 bar). The low pressure range was selected to extract the Henry's constants, for making a comparison with those obtained in our previous study³³ and also for computing the ideal selectivities, while the high

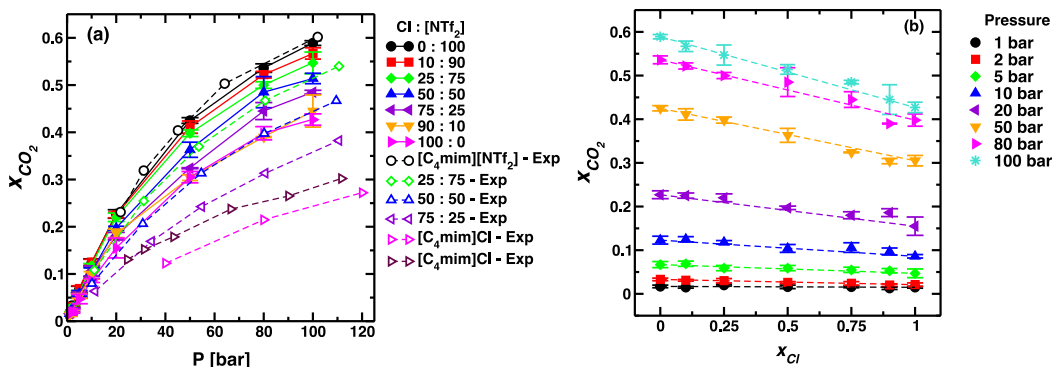


Figure 1. Solubilities of CO_2 in binary ionic liquid mixtures of $[\text{C}_4\text{mim}]\text{Cl}_x[\text{NTf}_2]_{1-x}$ at 353 K (a) shown as a function of different pressures of 1, 2, 5, 10, 20, 50, 80, and 100 bar; and (b) as a function of molar composition computed at a given pressure. Standard deviations were calculated from three independent trials for all mixture compositions. Note that the lines joining data points in (a) are only guides to the eye while dotted lines in (b) represent the mixing rule (eq 2). The available literature values for pure $[\text{C}_4\text{mim}]\text{Cl}$ are taken from Carvalho et al.,⁴¹ those for pure $[\text{C}_4\text{mim}]\text{Cl}$ are taken from Taguchi et al.,⁴³ and Jang et al.,⁴² while those for IL mixtures are taken from Hiraga et al.⁴⁴

182 pressure regime was probed to assess the nonideality of the gas
 183 absorption when mixtures are considered. CO_2 and CH_4 mixed
 184 gas solubilities were computed at 100 bar pressure with starting
 185 CO_2/CH_4 mole ratios of 05:95 and 15:85 in the gas phase. All
 186 the simulations were performed at a temperature of 353 K to
 187 ensure a liquid phase of ionic liquids used in this work and
 188 maintain consistency with our previous studies.^{32,33}

189 A system size consisting of 256 ion pairs was used for all the
 190 ionic liquid compositions, except at $x = 0.10$ and $x = 0.90$, for
 191 which 250 ion pairs were simulated. For pure gas solubilities,
 192 the ionic liquid phase was generated by randomly placing the
 193 ions in a three-dimensional periodic cubic box. The initial
 194 density of these systems was set identical to that obtained from
 195 our previous molecular dynamics study³² while the gas phase
 196 contained 500 molecules of either CO_2 or CH_4 molecules.
 197 Though the system size of the ionic liquid used for mixed gas
 198 solubilities remained the same, the number of CO_2/CH_4
 199 molecules were chosen as 100/1900 and 150/850 to reflect
 200 05:95 and 15:85 molar ratios in the gas phase. The initial
 201 configuration was prepared using CASSANDRA, employing a
 202 configurational bias methodology. The full description of the
 203 configurational bias algorithm implemented in CASSANDRA
 204 can be found elsewhere.⁴⁰ Briefly, conformational degrees of
 205 freedom of articulated molecules such as the cation $[\text{C}_4\text{mim}]^+$
 206 and $[\text{NTf}_2]^-$ are sampled by breaking the molecules in
 207 fragments. These fragments are generated in such a way that
 208 each fragment contains a branch point (atoms connected to
 209 more than one atom) and all the atoms bonded to it. Adjacent
 210 fragments share a common bond about which the relative
 211 orientations of the two fragments are sampled. For $[\text{C}_4\text{mim}]^+$,
 212 the imidazolium ring and the two carbon atoms connected to
 213 the ring constitute a fragment. For each of the fragments,
 214 100000 snapshots resulting from the sampling of bond angle
 215 distributions are generated prior to an actual simulation.
 216 During the course of a simulation, one of the samples is
 217 selected at random and the molecule is reassembled by placing
 218 the fragments one at a time. For the transfer of gas molecules,
 219 the configurational bias insertion method involves generating
 220 12 randomly selected trial positions for the placement of the
 221 gas molecule in the receiving box. In the case of CO_2 , the
 222 molecule is also given a random orientation. Out of the 12
 223 positions, a trial site is selected based on the Boltzmann weight
 224 of the van der Waals and electrostatic energy (for CO_2)

225 calculated with the atoms within 6.5 Å of the COM of the
 226 molecule.

227 A MC simulation consisted of moves to equalize temper-
 228 ature in each box, the pressure of the two boxes, and the
 229 chemical potential of the gases between the two phases. To
 230 achieve thermal equilibration, three types of MC moves were
 231 carried out: (i) translation of the center-of-mass (COM) of a
 232 molecule; (ii) rotation of the molecule about a randomly
 233 chosen axis (x , y , or z) with the COM placed at the origin; and
 234 (iii) conformational changes through a fragment-based
 235 sampling approach, as described above.⁴⁰ The probability of
 236 performing each of these moves was set to 30% for all the
 237 simulations. Pressure equilibration was ensured through the
 238 volume displacement moves, with a frequency of 0.5%. Unlike
 239 the constant volume GEMC, the volume displacement was
 240 carried out independently for each of the boxes. Due to the
 241 negligible vapor pressure of ionic liquids, only gas molecules
 242 were exchanged between the two phases to enforce the
 243 equality of chemical potential. Such particle transfer was
 244 attempted with 9.5% probability. The LJ and electrostatic
 245 interactions were truncated at 12 Å, consistent with the ionic
 246 liquid force field. Appropriate tail corrections were added to
 247 the LJ potential. The long-range component of the electrostatic
 248 interactions was calculated using the Ewald method. All the
 249 simulations were equilibrated for 25 million Monte Carlo (M
 250 MC) steps, followed by subsequent production runs of 50 M
 251 MC steps. The final 10 M MC steps were used to compute the
 252 averages. The statistical uncertainties were calculated by
 253 conducting three independent trials, where different initial
 254 configurations were obtained using different random seeds.

■ RESULTS AND DISCUSSION

255 **Pure Gas Absorption. CO_2 Solubility.** The CO_2 absorption isotherms at pressures ranging from 1 to 100 bar and the temperature of 353 K as a function of the anion composition are presented in Figure 1(a). Also included are the comparisons of the CO_2 solubilities obtained in this work with the available experimental data. The simulation results for CO_2 mole fractions in the $[\text{C}_4\text{mim}]\text{Cl}$ ionic liquid are predicted in excellent agreement with the experimental measurements,⁴¹ even at high pressures where it is known that the sampling becomes challenging²² due to high solubility of CO_2 . Simulation results also capture the experimentally

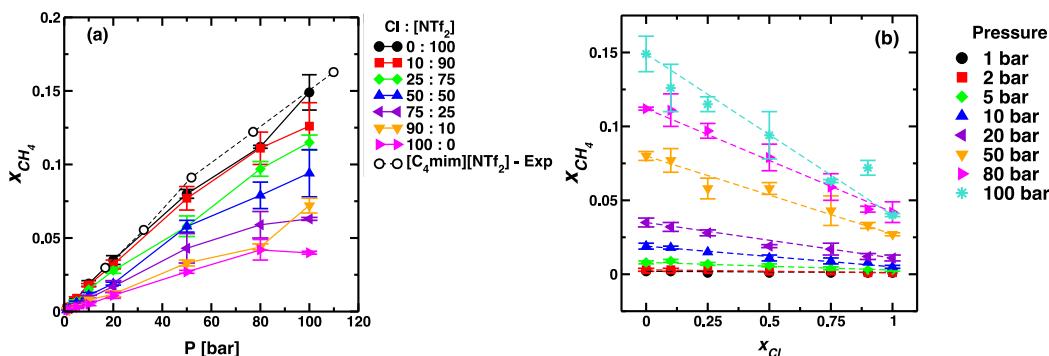


Figure 2. Solubilities of CH_4 in binary ionic liquid mixtures of $[\text{C}_4\text{mim}]\text{Cl}_x[\text{NTf}_2]_{1-x}$ at 353 K (a) shown as a function of different pressures of 1, 2, 5, 10, 20, 50, 80, 100 bar; and (b) as a function of molar composition computed at a given pressure. Standard deviations were calculated from three independent trials for all mixture compositions. Note that the lines joining data points in (a) are only guides to the eye while the dotted lines in (b) represent the mixing rule (eq 2). The available literature values for pure $[\text{C}_4\text{mim}]\text{Cl}$ are taken from Raeissi et al.¹⁷ for the same pressure range and temperature conditions, while the data for pure $[\text{C}_4\text{mim}]\text{Cl}$ for the same operating conditions is not available to the best of our knowledge.

267 observed nonlinear trend for CO_2 solubilities with pressure
268 such that the CO_2 mole fraction is a linear function of pressure
269 at low to moderate pressures and approaches an asymptotic
270 limit as the gas phase pressure is increased. This phenomenon
271 is related to a significant decrease in the void volume in the
272 ionic liquid with pressure.

273 A comparison of the CO_2 solubility data in $[\text{C}_4\text{mim}]\text{Cl}$
274 generated with simulations and those obtained experimentally
275 at high pressure suggests that the simulation results are
276 consistently higher than the experimental data.^{42–44} We
277 recently reported³³ a similar observation that the Henry's
278 constant for CO_2 in $[\text{C}_4\text{mim}]\text{Cl}$ calculated using the MD-BAR
279 approach was underpredicted relative to the experimental
280 values reported by Hiraga et al.,⁴⁴ suggesting that the
281 simulations predict low-pressure CO_2 solubilities in $[\text{C}_4\text{mim}]$
282 Cl that are higher than the experimental measurements. It is
283 conceivable that the difference arises due to the difficulties in
284 measuring CO_2 solubilities as $[\text{C}_4\text{mim}]\text{Cl}$ is viscous, and the
285 melting point of $[\text{C}_4\text{mim}]\text{Cl}$ is not too far from 353 K. In fact,
286 the experimental absorption isotherms included in Figure 1(a)
287 clearly demonstrate that a considerable variation in the
288 experimental measurements of CO_2 solubilities exists in this
289 ionic liquid.

290 The absorption isotherms for CO_2 in the binary ionic liquid
291 mixtures follow similar trends as noted for the pure ionic liquid
292 systems; that is, at low pressures the CO_2 mole fraction varies
293 linearly with the pressure while the CO_2 solubilities increase
294 sublinearly at moderate to high pressures. Furthermore, the
295 solubility of CO_2 at a given binary ionic liquid composition is
296 seen to be intermediate between the corresponding pure ionic
297 liquid CO_2 solubilities. To assess if the solubilities deviate from
298 the ideal mixing behavior, mole fractions of CO_2 are plotted
299 against the ionic liquid compositions in Figure 1(b) for
300 different pressures. The CO_2 mole fraction, on the basis of the
301 ideal mixing rule, can be calculated as

$$302 \quad x_{\text{ideal}} = x_1 X_1 + x_2 X_2 \quad (2)$$

303 and is depicted as dotted lines in Figure 1(b). In eq 2, x_1 and
304 x_2 refer to the mole fraction of CO_2 in pure ionic liquid; X_1 and
305 X_2 denote the mole fractions of the ionic liquids on a CO_2 -free
306 basis. It is clearly evident that the solubilities are weakly
307 dependent on the molar compositions of the ionic liquid
308 mixtures at pressures below 10 bar. In this regime, the CO_2
309 mole fractions in binary ionic liquid mixtures can be accurately

predicted by the ideal mixing rule (eq 2), which is consistent
310 with our previous study demonstrating that the Henry's
311 constants for CO_2 in this binary ionic liquid system can be
312 approximated from the knowledge of the Henry's constants
313 obtained for the pure ionic liquids.³³ As the pressure is
314 increased, deviations from the ideal mixing behavior begin to
315 appear. For example, CO_2 solubilities are consistently higher
316 than those suggested by the ideal mixing behavior at 20 bar.
317 Solubilities in excess to the ideal mixing values were also
318 observed for higher pressures, especially for the ionic liquid
319 mixture lean in $[\text{NTf}_2]^-$ ($x_{\text{Cl}} > 0.50$).
320,33

321 In our previous studies,^{32,33} we showed that the $[\text{NTf}_2]^-$
322 anion is displaced from its favorable hydrogen bonding
323 interaction, along the C–H vector, involving the most acidic
324 imidazolium ring hydrogen in the ionic liquid mixtures; the
325 positions above and below the plane of the imidazolium ring
326 become more populated as the concentration of Cl^- increases.
327 The rearrangement of $[\text{NTf}_2]^-$ is likely to enable an enhanced
328 interaction between the CO_2 molecules and the $[\text{NTf}_2]^-$
329 anion. We believe that the presence of such non-native
330 structures in $[\text{C}_4\text{mim}] \text{Cl}_x [\text{NTf}_2]_{1-x}$ ionic liquid mixtures is
331 one of the major contributing factors for the deviation of CO_2
332 solubilities from the ideal mixing rule. Furthermore, at higher
333 pressures, a slight reorientation of ion moieties can be
334 expected. Zhao et al.⁴⁵ showed a marked conformation
335 transition of the butyl chain of $[\text{C}_4\text{mim}]^+$ from anti to gauche
336 under very high pressures. Our previous work³³ suggested that
337 CO_2 approaches the cation majorly from the alkyl chain side.
338 Thus, the conformation change of alkyl chain can further aid
339 better CO_2 absorption, plausibly leading to the nonideality.
339

340 **CH_4 Solubility.** The CH_4 solubilities computed at different
341 pressures and 353 K, as a function of Cl^- composition, are
342 reported in Figure 2(a). The computed CH_4 absorption
343 isotherm for $[\text{C}_4\text{mim}]\text{Cl}$ in this work agrees well with that
344 determined by Raeissi et al.¹⁷ over the entire pressure range.
345 To the best of our knowledge, no experimental data exists for
346 CH_4 solubilities in $[\text{C}_4\text{mim}]\text{Cl}$ for comparing the CH_4
347 solubility predictions. The solubility of CH_4 in the pure ionic
348 liquid systems is lower than the corresponding CO_2
349 solubilities. On the contrary to the nonlinear behavior of
350 CO_2 absorption isotherms with pressure, the CH_4 solubilities
351 exhibit linearity over a larger pressure range. In general, the
352 solubilities of CH_4 in the mixtures are bracketed by those in
353 the pure ionic liquids.
353

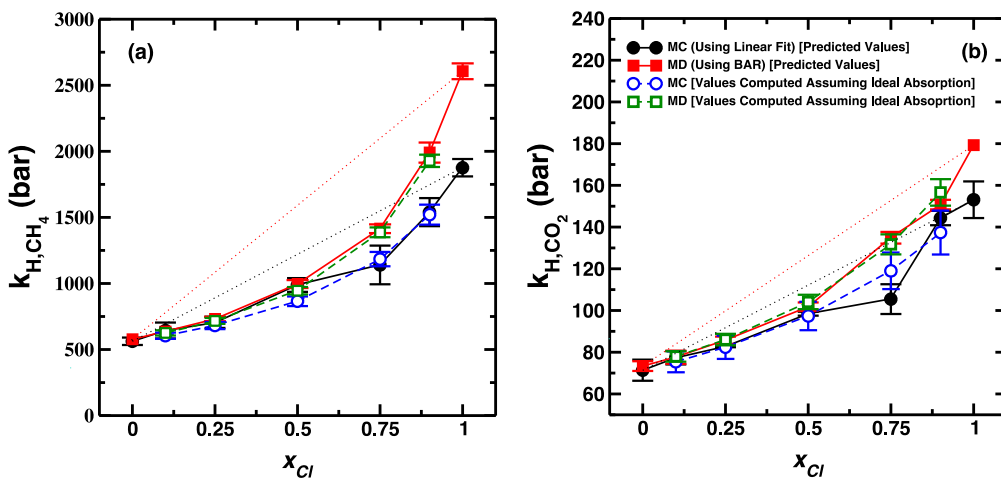


Figure 3. Comparison of Henry's constants of (a) CH_4 and (b) CO_2 calculated using MC simulations and those computed using the BAR technique employed in MD simulations for the mixture system of $[\text{C}_4\text{mim}]\text{Cl}_x[\text{NTf}_2]_{1-x}$. Standard deviations were calculated from three independent trials for all mixture compositions. Note that the lines joining data points are only guides to the eye while dotted lines represent the linear mixing rule. The values for CO_2 -MD(BAR) are taken from our previous work.³³

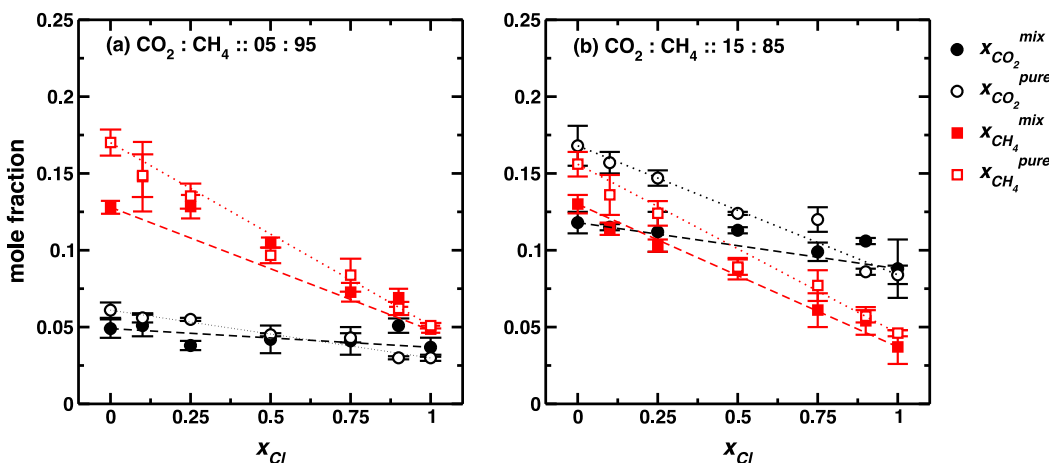


Figure 4. CO_2/CH_4 gas mixture solubility in a binary IL mixture of $[\text{C}_4\text{mim}]\text{Cl}_x[\text{NTf}_2]_{1-x}$ as a function of molar composition computed at 353 K and total pressure of 100 bar compared with pure gas solubilities of CO_2 and CH_4 at 100 bar, respectively, (a) for the gas phase mixture ratio of $\text{CO}_2/\text{CH}_4::05/95$; and (b) for the gas phase mixture ratio of $\text{CO}_2/\text{CH}_4::15/85$. Standard deviations were calculated from three independent trials for all mixture compositions. Note that the dotted lines represent the mixing rule (eq 2).

The absorption data for CH_4 are plotted as a function of the Cl^- composition in Figure 2(b) to uncover deviations from the linear mixing rule (eq 2). The low pressure behavior ($P < 20$ bar) is accurately described by the linear mixing rule. Small departures from ideality are noted at $P = 20$ bar. However, the small solubilities and the associated statistical uncertainties make it challenging to identify ionic liquid compositions at which CH_4 solubility deviates significantly from the linear mixing rule. It is only at $P = 100$ bar and the Cl^- - $[\text{NTf}_2]$ mole ratio of 90:10 that there is a statistically significant enhancement in CH_4 solubility in comparison to the ideal behavior.

Henry's Constants. Henry's constants can be obtained from the absorption isotherms by taking a linear fit as pressure tends to zero. Figure S2 of the Supporting Information illustrates the linear fit process for the calculation of Henry's constants of

CH_4 in $[\text{C}_4\text{mim}][\text{NTf}_2]$ ionic liquid. This procedure has been applied on each independent simulation trial to obtain the average Henry's constant values and the statistical uncertainties. However, as the isotherms have a nonlinear curvature, it is important to mention that Henry's constant values are heavily dependent on the range of data used for linear fit due to the curvature at high pressures. In this study, for CO_2 , the data range is chosen based on the observed solubility value and, hence, is not the same for all the systems studied in this work. However, the data-range has been included in Table S3 of the Supporting Information, to help the reader reproduce the results if desired. On the contrary, due to very low CH_4 solubility, linear fits from $P = 0$ up to $P = 50$ bar are taken to calculate Henry's constants. This range is justified as the computed Henry's constant for CH_4 in $[\text{C}_4\text{mim}][\text{NTf}_2]$ is 560

384 bar (see Table S4, Supporting Information), which is close to 385 the 541 bar determined experimentally from a linear fit of the 386 solubility data between 15.9 to 50 bar.¹⁷ As all the other ionic 387 liquid mixtures exhibit CH₄ solubility lower than that found for 388 [C₄mim][NTf₂], the pressure range is adequate to extract the 389 Henry's constants. We also performed infinitely dilute 390 solvation free energy calculations for CH₄ with molecular 391 dynamics simulations, employing the Bennett acceptance ratio 392 (BAR) approach, represented as the MD-BAR technique in 393 this work. The simulation protocol for these calculations is 394 provided in the Supporting Information. The Henry's 395 constants for CO₂ computed with MD-BAR are directly 396 taken from our previous work.³³

397 Figure 3 reports a comparison of the Henry's constants 398 calculated using both GEMC and MD-BAR techniques for the 399 gases along with the values estimated based on the Henry's 400 constants in [C₄mim][NTf₂] and [C₄mim]Cl according to eq 401 3 for the ionic liquid-ionic liquid mixtures.

$$402 \quad \frac{1}{H_{\text{mix}}} = \frac{X_1}{H_1} + \frac{X_2}{H_2} \quad (3)$$

403 For both the gases, the Henry's constants are strongly 404 dependent on the molar compositions of the ionic liquid 405 mixtures. Furthermore, it is seen that, within the statistical 406 uncertainty, the linear mixing rule (eq 3) provides a reasonable 407 approximation to the computed value at any given ionic liquid 408 composition, regardless of the simulation technique used.

409 **CO₂/CH₄ Mixture Solubility.** Solubilities of CO₂/CH₄ gas 410 mixtures in the binary ionic liquid mixture of [C₄mim] Cl_x 411 [NTf₂]_{1-x} at 353 K and a total pressure of 100 bar were 412 calculated for CO₂:CH₄ starting gas phase mole ratios of 05:95 413 and 15:85. The objective of this work was to determine if the 414 two gases absorb independently. Additionally, it was also 415 intended to discern the influence of nonideality in the 416 molecular structures of the ionic liquid mixtures on the 417 selectivity of CO₂ over CH₄.

418 Figure 4 presents the liquid phase compositions of CO₂ and 419 CH₄ for the two starting gas phase mole ratios. Also included 420 in this figure are the ideal liquid phase mole fractions of the 421 two solutes estimated using Henry's law at the equilibrium gas 422 phase partial pressures. The approach is justified because the 423 partial pressures of CO₂ are low enough to be in the Henry's 424 law regime. Similarly, the CH₄ solubility is described by 425 Henry's law up to the pressures considered in this work. For 426 pure [C₄mim][NTf₂] ionic liquid, the amount of CO₂ 427 absorbed for both the CO₂:CH₄ gas phase mole ratios of 428 05:95 and 15:85 is lower than that observed in the pure CO₂ 429 gas system. Similar observations are made for CH₄ solubility. 430 These trends suggest competitive absorption of the two gases. 431 From a molecular perspective, the observation also indicates 432 that a fraction of favorable interaction sites are common 433 between CO₂ and CH₄. Our results for CH₄ solubility in the 434 05:95 mixture are in contrast to those reported by Budhathoki 435 et al.²² for the CO₂:CH₄ gas phase mole ratio of 04:96. The 436 authors observed that while the solubility of CO₂ decreased 437 relative to the pure CO₂ system, the amount of CH₄ was 438 slightly higher than that for the pure CH₄ system, implying 439 enhanced CH₄ absorption in the presence of CO₂. However, 440 the competitive absorption mechanism is consistent between 441 this work and that of Budhathoki et al.²² when the starting 442 CO₂ mole fraction increases in the gas phase. Unlike pure 443 [C₄mim][NTf₂] ionic liquid, the mixed gas solubilities of both

444 CO₂ and CH₄ are similar to the pure gas solubilities in the pure 445 [C₄mim]Cl system, independent of their mole ratios. 445

446 Results from Monte Carlo (MC) simulations of mixture 447 absorption and ideal gas solubility computation for the starting 448 gas-phase mole ratio of 05:95 are presented in Figure 4(a) for 449 the entire ionic liquid composition range. It can be seen that 449 the MC results for CH₄ mole fractions in various ionic liquid 450 mixtures are close to those predicted assuming ideal mixing 451 except for the pure [C₄mim][NTf₂] ionic liquid. On the other 452 hand, the MC estimates of CO₂ solubilities can be 453 approximated by the solubilities computed using ideal mixing 454 behavior except when x_{Cl} = 0.90. We believe that this is due to 455 the presence of non-native arrangement of the two anions 456 around the cation as reported in our earlier publications.^{32,33} 457 Also, a consistent overlap of mixed gas CH₄ solubilities and the 458 pure CH₄ gas solubilities across the entire composition range 459 indicates that the presence of highly soluble gas CO₂ and the 460 composition of the ionic liquid mixture do not lead to 461 enhancement in the solubility of CH₄. 462

463 The equilibrium liquid-phase compositions of CO₂ and CH₄ 463 for the starting gas-phase mole ratio of 15:85 at 100 bar are 464 presented in Figure 4(b). We notice that the mole fraction of 465 CO₂ in various ionic liquid mixtures steadily decreases as the 466 concentration of Cl⁻ increases. A similar trend is observed for 467 the liquid-phase mole fractions predicted from MC simulations 468 for CH₄. For both the gases, the MC results consistently fall 469 below those suggested by the ideal solubility calculations for 470 x_{Cl} < 0.50, implying that the competitive absorption is 471 dominant when Cl⁻ is the minority component. For equimolar 472 and higher Cl⁻ concentrations, the MC calculations of mixture 473 solubilities are well reproduced using the ideal solubility 474 mechanism except for x_{Cl} = 0.90. Although the mixture 475 solubilities closely follow the ideal gas solubility calculations, 476 we stress that the physical dissolution mechanism of these 477 gases is likely to be distinct from those in the pure ionic liquid. 478 For example, we demonstrated that the Henry's constant of 479 CO₂ in the same binary ionic liquid mixtures could be 480 estimated using the ideal mixing behavior for the pure ionic 481 liquid Henry's constants for CO₂, yet the CO₂ absorption 482 mechanism is different, especially for ionic liquid mixtures rich 483 in Cl⁻.³³ Higher solubility of CO₂ at x_{Cl} = 0.90 than the ideal 484 solubility is probably due to "free" [NTf₂]⁻ in the system at 485 this concentration.^{32,33} 486

487 **Solubility Selectivity.** To account for the trends observed 487 in mixed gas absorption isotherms, solubility selectivities were 488 computed. Two different methods were employed. In the first 489 method, solubility selectivities were directly calculated from 490 the liquid and the gas phase compositions of the corresponding 491 components obtained from the MC simulations as shown in eq 492 4

$$493 \quad \beta_{\text{CO}_2/\text{CH}_4}^{\text{S}} = \left(\frac{x_{\text{CO}_2}/y_{\text{CO}_2}}{x_{\text{CH}_4}/y_{\text{CH}_4}} \right)_{P,T} \quad (4) \quad 494$$

495 where x and y are the mole fractions in the liquid and gas 495 phase, respectively, while the ideal solubility selectivities were 496 determined by taking the ratio of Henry's constants, for a 497 specific ionic liquid mixture, as shown in eq 5 498

$$499 \quad \beta_{\text{CO}_2/\text{CH}_4}^{\text{S,ideal}} = \left(\frac{k_{\text{H,CH}_4}}{k_{\text{H,CO}_2}} \right) \quad (5) \quad 499$$

500 The mixture selectivities computed via eq 4 for the two
 501 starting gas-phase mole ratios of $\text{CO}_2:\text{CH}_4$ are displayed in
 502 Figure 5 along with the ideal selectivity obtained from eq 5.

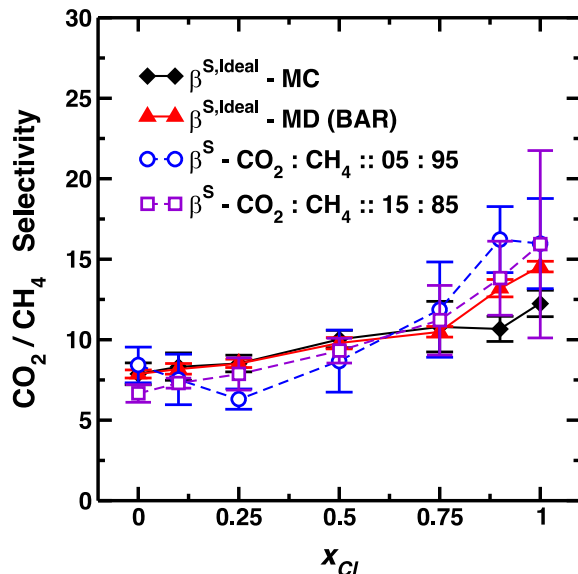


Figure 5. Comparison of CO_2/CH_4 gas mixture solubility selectivities ($\beta_{\text{CO}_2/\text{CH}_4}^S$), with $\text{CO}_2:\text{CH}_4$ gas phase mole ratios of 05:95 and 15:85, in binary IL mixture of $[\text{C}_4\text{mim}]\text{Cl}_x[\text{NTf}_2]_{1-x}$ as a function of molar composition computed at 353 K and total pressure of 100 bar with ideal solubility selectivities ($\beta_{\text{CO}_2/\text{CH}_4}^{\text{S,ideal}}$) computed using the ratio of Henry's law constants using both GEMC and BAR techniques. Standard deviations were calculated from three independent trials for all mixture compositions. Note that the lines joining data points are only guides to the eye.

using both GEMC and MD-BAR methods are in very good 506 agreement. The ideal selectivities range from ~ 8 to ~ 12 in 507 going from the pure $[\text{C}_4\text{mim}]\text{[NTf}_2]$ to pure $[\text{C}_4\text{mim}]\text{Cl}$. The 508 increase in the selectivity is due to a less dramatic effect of the 509 ionic liquid composition on the Henry's constant of CO_2 than 510 that for CH_4 . This is clearly borne out by nonlinear behavior of 511 ideal selectivity as a function of ionic liquid composition. 512 Further, the ideal solubility selectivity of ~ 8 for pure ionic 513 liquid $[\text{C}_4\text{mim}]\text{[NTf}_2]$ is comparable to the experimental 514 selectivity value of ~ 7 published by Ramdin et al.⁴⁶ at the same 515 temperature condition. The ideal selectivity is also comparable 516 to 7.9 ± 0.5 reported by Budhathoki et al. for $[\text{C}_4\text{mim}]\text{[NTf}_2]$ 517 at 333 K.²²

For pure $[\text{C}_4\text{mim}]\text{[NTf}_2]$ ionic liquid, the computed 519 mixture solubility selectivity ($\beta_{\text{CO}_2/\text{CH}_4}^S$) for the mole ratio of 520 05:95 is roughly equal to the ideal solubility selectivity 521 computed from the ratio of the Henry's constants ($\beta_{\text{CO}_2/\text{CH}_4}^{\text{S,ideal}}$), 522 whereas for the gas phase mole ratios of 15:85 the mixture 523 solubility selectivity is lower than the ideal solubility selectivity. 524 On the other hand, the mixture solubility selectivity in the pure 525 $[\text{C}_4\text{mim}]\text{Cl}$ for both the starting gas-phase mole ratios can be 526 estimated with the ideal selectivity assumption. In fact, for the 527 entire composition range of ionic liquid mixtures the ideal 528 assumption for the prediction of solubility selectivity seems to 529 be irrespective of the gas-phase mole ratios except at $x_{\text{Cl}} = 0.90$ 530 for 05:95 mol ratio. It is important to mention that the 531 statistical uncertainties were calculated from three independent 532 trials for all mixture compositions. A comparison of the 533 selectivity obtained for the mixtures at $x_{\text{Cl}} = 0.75$, 0.90, and 534 1.00 for three vs five independent runs, shown in Table 2, 535 t2 demonstrates that the selectivity is rather invariant with 536 increasing number of independent runs. However, the 537 uncertainty in, some instances, is lower when five independent 538 simulations are used. Nonetheless, results show that a small 539 amount of $[\text{C}_4\text{mim}]\text{[NTf}_2]$ in $[\text{C}_4\text{mim}]\text{Cl}$ (up to 10%) has the 540 potential to improve the gas separation performance of the 541 ionic liquid system, a result consistent with the gas mixture 542 solubility isotherms. Similar observations have been reported 543 previously for the enhancement in the solubility selectivity of 544 CO_2 over both CH_4 and N_2 by adding 5–10% of $[\text{C}_2\text{mim}]$ - 545

503 The calculated values are also collected in Table 1. It is evident
 504 that the ideal solubility selectivities ($\beta_{\text{CO}_2/\text{CH}_4}^{\text{S,ideal}}$) obtained for the
 505 binary ionic liquid mixtures of $[\text{C}_4\text{mim}]\text{Cl}_x[\text{NTf}_2]_{1-x}$ at 353 K

Table 1. CO_2/CH_4 Mole Percent Compositions in Liquid and Gas Phase and Solubility Selectivities in Binary Ionic Liquid Mixture of $[\text{C}_4\text{mim}]\text{Cl}_x[\text{NTf}_2]_{1-x}$ at 353 K and a Total Pressure of 100 bar^a

$\text{CO}_2:\text{CH}_4$	x_{IL}	x_{CO_2}	y_{CO_2}	x_{CH_4}	y_{CH_4}	β^S	$\beta^S, \text{ Ideal(MC)}$	$\beta^S, \text{ Ideal(MD)}$
05:95	0.00	0.049 ₆	0.044 ₁	0.128 ₄	0.956 ₁	8.43 ± 1.11	7.88 ± 0.68	7.87 ± 0.25
	0.10	0.051 ₇	0.043 ₁	0.148 ₂₃	0.957 ₁	7.53 ± 1.57	8.33 ± 0.85	8.19 ± 0.33
	0.25	0.038 ₃	0.045 ₀	0.128 ₈	0.955 ₀	6.31 ± 0.63	8.52 ± 0.52	8.53 ± 0.26
	0.50	0.042 ₉	0.045 ₁	0.105 ₃	0.955 ₁	8.67 ± 1.93	10.04 ± 0.54	9.78 ± 0.35
	0.75	0.041 ₉	0.045 ₁	0.073 ₆	0.955 ₁	11.87 ± 2.96	10.81 ± 1.57	10.49 ± 0.33
	0.90	0.051 ₅	0.044 ₁	0.069 ₆	0.956 ₁	16.22 ± 2.05	10.67 ± 0.78	13.20 ± 0.54
	1.00	0.037 ₆	0.045 ₁	0.049 ₂	0.955 ₁	15.97 ± 2.80	12.25 ± 0.82	14.54 ± 0.33
15:85	0.00	0.118 ₇	0.12 ₃	0.130 ₆	0.880 ₃	6.66 ± 0.55		
	0.10	0.115 ₂	0.122 ₁	0.114 ₄	0.878 ₁	7.30 ± 0.31		
	0.25	0.112 ₁₃	0.122 ₄	0.103 ₄	0.878 ₄	7.87 ± 1.00		
	0.50	0.113 ₂	0.122 ₁	0.088 ₇	0.878 ₁	9.32 ± 0.77		
	0.75	0.099 ₆	0.126 ₂	0.061 ₁₁	0.874 ₂	11.21 ± 2.16		
	0.90	0.106 ₂	0.124 ₁	0.054 ₉	0.876 ₁	13.82 ± 2.30		
	1.00	0.088 ₁₉	0.129 ₆	0.037 ₁₁	0.871 ₆	15.93 ± 5.82		

^ax and y represent mole percent compositions in the liquid and gas phase, respectively. Standard deviations are computed from three independent simulations. For composition data subscripts represent uncertainties. For example, $0.049_6 = 0.049 \pm 0.006$.

Table 2. Comparison of Selectivity (β^S) Values Obtained for the Mixtures at $x_{\text{Cl}} = 0.75, 0.90$, and 1.00 Using Three vs Five Independent Simulation Runs, at 353 K and a Total Pressure of 100 bar

$\text{CO}_2:\text{CH}_4$	x_{IL}	β^S (3 runs)	β^S (5 runs)
05:95	0.75	11.87 ± 2.96	12.94 ± 3.99
	0.90	16.22 ± 2.05	15.71 ± 1.62
	1.00	15.97 ± 2.80	14.89 ± 2.94
15:85	0.75	11.21 ± 2.16	10.91 ± 1.60
	0.90	13.82 ± 2.30	14.18 ± 3.44
	1.00	15.93 ± 5.82	15.87 ± 4.70

546 [NTf₂] in [C₂mim][BF₄].³⁴ The authors rationalized the 547 observation by suggesting lowering of the molar volume and a 548 slight disruption of the hydrogen bond network of pure 549 [C₂mim][BF₄] ionic liquid. The observations made in our 550 work in-part support the idea and provide further insight that 551 the disruption of the preferential hydrogen bonding network 552 leads to the possibility of nonideal structures, structures non- 553 native to pure ionic liquid analogues, that not only can help 554 improve the pure gas solubilities but also can enhance the 555 solubility selectivity of the mixture of gases.

556 ■ CONCLUSION

557 In this article, single component gas solubilities of CO₂ and 558 CH₄ were computed in the binary ionic liquid mixtures of 559 [C₄mim] Cl_x [NTf₂]_{1-x} ($x = 0.0, 0.10, 0.25, 0.50, 0.75, 0.90,$ 560 1.0) at 353 K and pressures ranging from 0 to 100 bar 561 computed using Gibbs ensemble Monte Carlo (GEMC) 562 simulations. In addition, mixture gas solubilities were also 563 determined for the starting gas-phase mole ratios of CO₂:CH₄ 564 of $05:95$ and $15:85$ at 100 bar . Henry's constants of CO₂ and 565 CH₄ were extracted from the single component absorption 566 isotherms and compared against the results obtained with free 567 energy calculations performed with MD-BAR. Selectivities of 568 CO₂ over CH₄ were calculated from the respective Henry's 569 constants and the mixture solubility data.

570 It was found that the solubility of CO₂ exhibited a linear 571 dependence at low pressures while the rate of increase of CO₂ 572 decreases as the pressure increased for the pure ionic liquids as 573 well as the mixtures. It was observed that the CO₂ solubilities 574 in the mixtures could be predicted from the solubility in the 575 pure ionic liquids up to a pressure of 20 bar using a linear 576 mixing rule. For higher pressures, nonideal behavior is noted 577 for CO₂ solubilities such that the predictions from the linear 578 mixing rule are consistently lower. The single-component 579 solubility of CH₄, on the other hand, shows linear dependence 580 on pressure up to 100 bar for all the ionic liquids examined in 581 this work. Furthermore, the solubility of CH₄ in the ionic 582 liquid mixtures is found to follow the ideal mixing rule, except 583 only at 100 bar pressure and $x_{\text{Cl}} = 0.90$.

584 CO₂:CH₄ gas mixture solubility data in the binary ionic 585 liquid mixtures of [C₄mim] Cl_x [NTf₂]_{1-x} suggest that, for the 586 CO₂:CH₄ gas phase mole ratio of $05:95$, the liquid-phase mole 587 fractions of the two gases can be predicted with reasonable 588 accuracy from the single-component absorption data. As the 589 initial amount of CO₂ in the gas phase is increased, for 590 example, the CO₂:CH₄ gas phase mole ratio of $15:85$, 591 competitive gas absorption mechanism is observed up to x_{Cl} 592 = 0.50 . Furthermore, despite a nonlinear trend in the solubility 593 selectivity with ionic liquid composition, the CO₂:CH₄ 594 selectivity is remarkably similar to the ideal selectivity for all

595 the systems, except for the $05:95$ mol ratio at $x_{\text{Cl}} = 0.90$, where 596 the selectivity observed was markedly higher than the ideal 597 selectivity.

598 ■ ASSOCIATED CONTENT

599 ■ Supporting Information

600 The Supporting Information is available free of charge on the 600 601 ACS Publications website at DOI: 10.1021/acs.iecr.9b03384. 601

602 Raw data at 353 K for CO₂ and CH₄ pure gas solubilities 602 603 at $P = 1, 2, 5, 10, 20, 50, 80, 100\text{ bar}$; mixed gas 603 604 solubilities with molar ratio of CO₂/CH₄ as $05:95$ and 604 605 $15:85$ in the gas phase and a total pressure of 100 bar ; 605 606 Henry's constants calculated using both Monte Carlo 606 607 and molecular dynamics BAR techniques; and solubility 607 608 selectivities; along with the chemical structure schematic 608 609 (PDF)

610 ■ AUTHOR INFORMATION

611 ■ Corresponding Author

612 *E-mail: jindal.shah@okstate.edu.

613 ■ ORCID ®

614 Utkarsh Kapoor: 0000-0002-4977-3405

615 Jindal K. Shah: 0000-0002-3838-6266

616 ■ Notes

617 The authors declare no competing financial interest.

618 ■ ACKNOWLEDGMENTS

619 J.K.S. would like to thank the Editors for extending the 619 620 invitation to contribute to the Charles Eckert Festschrift. We 620 621 also acknowledge Prof. Neeraj Rai and Prof. Sapna Sarupria for 621 622 useful discussions. This material is based upon work supported 622 623 by the National Science Foundation (NSF) Award Number 623 624 CBET-1706978. The authors gratefully acknowledge partial 624 625 funding from the Oklahoma State University. Computational 625 626 resources were provided by the High Performance Computing 626 627 Center (HPCC) at the Oklahoma State University.

628 ■ REFERENCES

- (1) Hao, J.; Rice, P. A.; Stern, S. A. Upgrading Low-Quality Natural 629 Gas With H₂S- And CO₂-Selective Polymer Membranes Part I. 630 Process Design And Economics of Membrane Stages Without Recycle 631 Streams. *J. Membr. Sci.* **2002**, *209*, 177–206.
- (2) Liu, Y.; Zhang, L.; Watanasiri, S. Representing Vapor–Liquid 633 Equilibrium for an Aqueous MEA–CO₂ System Using the Electrolyte 634 Nonrandom-Two-Liquid Model. *Ind. Eng. Chem. Res.* **1999**, *38*, 635 2080–2090.
- (3) Dupart, M. S.; Bacon, T. R.; Edwards, D. J. Understanding 637 Corrosion in Alkanolamine Gas Treating Plants. *Hydrocarbon* 638 Process. **1993**, *92*, 156–160.
- (4) Chang, H.; Shih, C. M. Simulation and Optimization for Power 640 Plant Flue Gas CO₂ Absorption-Stripping Systems. *Sep. Sci. Technol.* **2005**, *40*, 877–909.
- (5) Cadena, C.; Anthony, J. L.; Shah, J. K.; Morrow, T. I.; 643 Brennecke, J. F.; Maginn, E. J. Why is CO₂ So Soluble in 644 Imidazolium-Based Ionic Liquids? *J. Am. Chem. Soc.* **2004**, *126*, 645 5300–5308.
- (6) Lee, S.-H.; Kim, B.-S.; Lee, E.-W.; Park, Y.-I.; Lee, J.-M. The 647 Removal of Acid Gases From Crude Natural Gas By Using Novel 648 Supported Liquid Membranes. *Desalination* **2006**, *200*, 21–22.
- (7) Finotello, A.; Bara, J. E.; Camper, D.; Noble, R. D. Room- 650 Temperature Ionic Liquids: Temperature Dependence of Gas 651 Solubility Selectivity. *Ind. Eng. Chem. Res.* **2008**, *47*, 3453–3459.
- (8) Ramdin, M.; Balaji, S. P.; Vicent-Luna, J. M.; Gutiérrez-Sevillano, 653 J. J.; Calero, S.; de Loos, T. W.; Vlugt, T. J. H. Solubility of the 654

655 Precombustion Gases CO_2 , CH_4 , CO , H_2 , N_2 , and H_2S in the Ionic
656 Liquid $[\text{bmim}][\text{Tf}_2\text{N}]$ from Monte Carlo Simulations. *J. Phys. Chem. C* 2014, 118, 23599–23604.

658 (9) Anderson, J. L.; Dixon, J. K.; Brennecke, J. F. Solubility of CO_2 ,
659 CH_4 , C_2H_6 , C_2H_4 , O_2 , and N_2 in 1-Hexyl-3-methylpyridinium
660 Bis(trifluoromethylsulfonyl)imide: Comparison to Other Ionic
661 Liquids. *Acc. Chem. Res.* 2007, 40, 1208–1216.

662 (10) Anthony, J. L.; Maginn, E. J.; Brennecke, J. F. Solubilities and
663 Thermodynamic Properties of Gases in the Ionic Liquid 1-n-Butyl-3-
664 methylimidazolium Hexafluorophosphate. *J. Phys. Chem. B* 2002, 106,
665 7315–7320.

666 (11) Blanchard, L. A.; Brennecke, J. F. Green Processing using Ionic
667 Liquids and CO_2 . *Nature* 1999, 399, 1–2.

668 (12) Hojniak, S. D.; Silverwood, I. P.; Khan, A. L.; Vankelecom, I. F.
669 J.; Dehaen, W.; Kazarian, S. G.; Binnemans, K. Highly Selective
670 Separation of Carbon Dioxide from Nitrogen and Methane by
671 Nitrile/Glycol-Difunctionalized Ionic Liquids in Supported Ionic
672 Liquid Membranes (SILMs). *J. Phys. Chem. B* 2014, 118, 7440–7449.

673 (13) Shahkaramipour, N.; Adibi, M.; Seifkordi, A. A.; Fazli, Y.
674 Separation of CO_2/CH_4 Through Alumina-Supported Geminal Ionic
675 Liquid Membranes. *J. Membr. Sci.* 2014, 455, 229–235.

676 (14) Bara, J. E.; Gabriel, C. J.; Hatakeyama, E. S.; Carlisle, T. K.;
677 Lessmann, S.; Noble, R. D.; Gin, D. L. Improving CO_2 Selectivity in
678 Polymerized Room-Temperature Ionic Liquid Gas Separation
679 Membranes Through Incorporation of Polar Substituents. *J. Membr. Sci.* 2008, 321, 3–7.

680 (15) Yokozeki, A.; Shiflett, M. B. Vapor–Liquid Equilibria of
682 Ammonia+Ionic Liquid Mixtures. *Appl. Energy* 2007, 84, 1258–1273.

683 (16) Yokozeki, A.; Shiflett, M. B. Hydrogen Purification Using
684 Room-Temperature Ionic Liquids. *Appl. Energy* 2007, 84, 351–361.

685 (17) Raeissi, S.; Peters, C. J. High Pressure Phase Behaviour of
686 Methane in 1-Butyl-3-Methylimidazolium Bis-
687 (Trifluoromethylsulfonyl)Imide. *Fluid Phase Equilib.* 2010, 294, 67–
688 71.

689 (18) Anderson, J. L.; Dixon, J. K.; Maginn, E. J.; Brennecke, J. F.
690 Measurement of SO_2 Solubility in Ionic Liquids. *J. Phys. Chem. B* 2006, 110, 15059–15062.

691 (19) Shiflett, M. B.; Yokozeki, A. Chemical Absorption of Sulfur
693 Dioxide in Room-Temperature Ionic Liquids. *Ind. Eng. Chem. Res.* 2010, 49, 1370–1377.

695 (20) Hert, D. G.; Anderson, J. L.; Aki, S. N. V. K.; Brennecke, J. F.
696 Enhancement of Oxygen and Methane Solubility in 1-Hexyl-3-
697 Methylimidazolium Bis(Trifluoromethylsulfonyl) Imide Using Car-
698 bon Dioxide. *Chem. Commun.* 2005, 39, 2603–3.

699 (21) Shi, W.; Sorescu, D. C.; Luebke, D. R.; Keller, M. J.;
700 Wickramanayake, S. Molecular Simulations and Experimental Studies
701 of Solubility and Diffusivity for Pure and Mixed Gases of H_2 , CO_2 ,
702 and Ar Absorbed in the Ionic Liquid 1-n-Hexyl-3-methylimidazolium
703 Bis(Trifluoromethylsulfonyl)amide ($[\text{hmim}][\text{Tf}_2\text{N}]$). *J. Phys. Chem. B* 2010, 114, 6531–6541.

705 (22) Budhathoki, S.; Shah, J. K.; Maginn, E. J. Molecular Simulation
706 Study of the Solubility, Diffusivity and Permselectivity of Pure and
707 Binary Mixtures of CO_2 and CH_4 in the Ionic Liquid 1-n-Butyl-3-
708 methylimidazolium bis(trifluoromethylsulfonyl)imide. *Ind. Eng. Chem. Res.* 2015, 54, 8821–8828.

710 (23) Budhathoki, S.; Shah, J. K.; Maginn, E. J. Molecular Simulation
711 Study of the Performance of Supported Ionic Liquid Phase Materials
712 for the Separation of Carbon Dioxide from Methane and Hydrogen.
713 *Ind. Eng. Chem. Res.* 2017, acs.iecr.7b00763-10, 56, 6775.

714 (24) Shi, W.; Maginn, E. J. Atomistic Simulation of the Absorption
715 of Carbon Dioxide and Water in the Ionic Liquid 1-n-Hexyl-3-
716 methylimidazolium Bis(trifluoromethylsulfonyl)imide ($[\text{hmim}][\text{Tf}_2\text{N}]$). *J. Phys. Chem. B* 2008, 112, 2045–2055.

718 (25) Lei, Z.; Dai, C.; Chen, B. Gas Solubility in Ionic Liquids. *Chem. Rev.* 2014, 114, 1289–1326.

720 (26) Shiflett, M. B.; Niehaus, A. M. S.; Yokozeki, A. Separation of
721 N_2O and CO_2 Using Room-Temperature Ionic Liquid $[\text{bmim}][\text{BF}_4]$.
722 *J. Phys. Chem. B* 2011, 115, 3478–3487.

727 (27) Shiflett, M. B.; Niehaus, A. M. S.; Yokozeki, A. Separation of
728 CO_2 and H_2S Using Room-Temperature Ionic Liquid $[\text{bmim}][\text{MeSO}_4]$. *J. Chem. Eng. Data* 2010, 55, 4785–4793.

729 (28) Solinas, M.; Pfaltz, A.; Cozzi, P. G.; Leitner, W. Enantioselective
730 Hydrogenation of Imines in Ionic Liquid/Carbon Dioxide Media. *J. Am. Chem. Soc.* 2004, 126, 16142–16147.

731 (29) Toussaint, V. A.; Kühne, E.; Shariati, A.; Peters, C. J. Solubility
732 Measurements of Hydrogen In 1-Butyl-3-Methylimidazolium Tetra-
733 fluoroborate and The Effect of Carbon Dioxide and A Selected
734 Catalyst On The Hydrogen Solubility in The Ionic Liquid. *J. Chem. Thermodyn.* 2013, 59, 239–242.

735 (30) Shi, W.; Maginn, E. J. Molecular Simulation and Regular
736 Solution Theory Modeling of Pure and Mixed Gas Absorption in the
737 Ionic Liquid 1-n-Hexyl-3-methylimidazolium Bis-
738 (Trifluoromethylsulfonyl)amide ($[\text{hmim}][\text{Tf}_2\text{N}]$). *J. Phys. Chem. B* 2008, 112, 16710–16720.

739 (31) Baltus, R. E.; Culbertson, B. H.; Dai, S.; Luo, H.; DePaoli, D. W. Low-Pressure Solu-
740 bility of Carbon Dioxide in Room-Temper-
741 ature Ionic Liquids Measured with a Quartz Crystal Microbalance. *J. Phys. Chem. B* 2004, 108, 721–727.

742 (32) Kapoor, U.; Shah, J. K. Preferential Ionic Interactions and
743 Microscopic Structural Changes Drive Nonideality in Binary Ionic
744 Liquid Mixtures as Revealed from Molecular Simulations. *Ind. Eng. Chem. Res.* 2016, 55, 13132–13146.

745 (33) Kapoor, U.; Shah, J. K. Molecular Origins of the Apparent Ideal
746 CO_2 Solubilities in Binary Ionic Liquid Mixtures. *J. Phys. Chem. B* 2018, 122, 9763–9774.

747 (34) Finotello, A.; Bara, J. E.; Narayan, S.; Camper, D.; Noble, R. D. Ideal Gas Solubilities and Solubility Selectivities in a Binary Mixture
750 of Room-Temperature Ionic Liquids. *J. Phys. Chem. B* 2008, 112, 752 2335–2339.

751 (35) Potoff, J. J.; Siepmann, J. I. Vapor-Liquid Equilibria of Mixtures
752 Containing Alkanes, Carbon Dioxide, and Nitrogen. *AIChE J.* 2004, 50, 1676–1682.

753 (36) Liu, Z.; Chen, T.; Bell, A.; Smit, B. Improved United-Atom
754 Force Field for 1-Alkyl-3-methylimidazolium Chloride. *J. Phys. Chem. B* 2010, 114, 4572–4582.

755 (37) Zhong, X.; Liu, Z.; Cao, D. Improved Classical United-Atom
756 Force Field for Imidazolium-Based Ionic Liquids: Tetrafluoroborate,
757 Hexafluorophosphate, Methylsulfate, Trifluoromethylsulfonate, Ac-
758 etate, Trifluoroacetate, and Bis(trifluoromethylsulfonyl)amide. *J. Phys. Chem. B* 2011, 115, 10027–10040.

759 (38) Kapoor, U.; Banerjee, A.; Shah, J. K. Evaluation of the
760 Predictive Capability of Ionic Liquid Force Fields for CH_4 , CO_2 , NH_3 ,
761 and SO_2 Phase Equilibria. *Fluid Phase Equilib.* 2019, 492, 161–173.

762 (39) Shah, J. K.; Marin-Rimoldi, E.; Mullen, R. G.; Keene, B. P.;
763 Khan, S.; Paluch, A. S.; Rai, N.; Romaniello, L. L.; Rosch, T. W.; Yoo,
764 B.; et al. Cassandra: An Open Source Monte Carlo Package For
765 Molecular Simulation. *J. Comput. Chem.* 2017, 38, 1727–1739.

766 (40) Shah, J. K.; Maginn, E. J. A General And Efficient Monte Carlo
767 Method For Sampling Intramolecular Degrees of Freedom of
768 Branched and Cyclic Molecules. *J. Chem. Phys.* 2011, 135, 134.

769 (41) Carvalho, P. J.; Alvarez, V. H.; Marrucho, I. M.; Aznar, M.;
770 Coutinho, J. A. P. High Pressure Phase Behavior of Carbon Dioxide in
771 1-Butyl-3-Methylimidazolium Bis(Trifluoromethylsulfonyl)Imide and
772 1-Butyl-3-Methylimidazolium Dicyanamide Ionic Liquids. *J. Supercrit. Fluids* 2009, 50, 105–111.

773 (42) Jang, S.; Cho, D.-W.; Im, T.; Kim, H. High-Pressure Phase
774 Behavior of CO_2 + 1-Butyl-3-Methylimidazolium Chloride System.
775 *Fluid Phase Equilib.* 2010, 299, 216–221.

776 (43) Taguchi, R. Measurement and Calculation of High Pressure
777 CO_2 Solubilities in Functional Ionic Liquids. *M.S. Thesis*, Graduate
778 School of Environmental Studies, Tohoku University, 2009.

779 (44) Hiraga, Y.; Koyama, K.; Sato, Y.; Smith, R. L., Jr. Measurement
780 and Modeling of CO_2 Solubility in $[\text{bmim}]\text{Cl}$ – $[\text{bmim}][\text{Tf}_2\text{N}]$
781 Mixed-Ionic Liquids For Design of Versatile Reaction Solvents. *J. Supercrit. Fluids* 2018, 132, 42–50.

782 (45) Zhao, Y.; Liu, X.; Lu, X.; Zhang, S.; Wang, J.; Wang, H.; Gurau,
783 Rogers, R. D.; Su, L.; Li, H. The Behavior of Ionic Liquids under
784

792 High Pressure: A Molecular Dynamics Simulation. *J. Phys. Chem. B*
793 2012, 116, 10876–10884.
794 (46) Ramdin, M.; Amplianitis, A.; de Loos, T. W.; Vlugt, T. J. H.
795 Solubility of CO₂/CH₄ Gas Mixtures in Ionic Liquids. *Fluid Phase*
796 *Equilib.* 2014, 375, 134–142.